

Adsorption of a water molecule on Fe(100): Density-functional calculations

Sung Chul Jung and Myung Ho Kang

Department of Physics, Pohang University of Science and Technology, Pohang 790-784, Korea

(Received 14 December 2009; published 29 March 2010)

Molecular and dissociative adsorption of a single water molecule on the Fe(100) surface has been studied by using density-functional theory calculations. We found that there exists a locally stable molecular adsorption state with an adsorption energy of 0.39 eV, where the H₂O molecule adsorbs on top of a surface Fe atom in a flat-lying molecular configuration. This molecular configuration is found to well reproduce the water-induced vibrational frequencies measured in a low-temperature electron-energy-loss spectroscopy (EELS) study. The H₂O molecular state is subject to a dissociation into H+OH species with an activation barrier of 0.35 eV. A further dissociation of the OH group into H+O species requires a higher activation energy of 0.79 eV. The prediction of the H₂O molecular precursor and the energy diagram for its dissociation is in good accordance with the adsorption picture which was suggested in a previous EELS study but has been incompatible with a previous density-functional study predicting a barrierless H+OH dissociation of water molecule.

DOI: [10.1103/PhysRevB.81.115460](https://doi.org/10.1103/PhysRevB.81.115460)

PACS number(s): 68.43.Bc, 68.43.Fg, 68.47.De

I. INTRODUCTION

Water-induced oxidation of iron surfaces is of great importance in corrosion, catalysis, and electrochemistry. Its initial stages involve the surface adsorption of water molecules, their dissociation into H+OH, and the further dissociation of OH into H+O. Atomistic details of these reactions are thus essential in understanding the initial stages of the water-induced oxidation of iron surfaces. Especially, in connection with the reaction kinetics, it is a question of fundamental importance whether there exist locally stable molecular adsorption states, being precursors to more stable dissociation states.¹⁻³

As a simple low-index face, the Fe(100) surface has long been used as a prototypical substrate for studying the interaction of water molecules with iron surfaces. Despite experimental and theoretical studies, however, it still remains unresolved whether the Fe(100) surface supports molecular precursor states or not. In an early Auger electron spectroscopy and low-energy electron-diffraction study of the H₂O/Fe(100) surface, Dwyer *et al.*⁴ proposed a reaction model involving a molecular precursor as a way of accounting for the observed temperature dependence of the oxygen coverage versus water exposure. Later, in their electron-energy-loss spectroscopy (EELS) and temperature programmed desorption (TPD) study, Hung *et al.*⁵ provided more evidence of water molecules on Fe(100) by assigning the EELS peaks measured at 100 K for a range of water exposures of 0.05–1.2 L to molecularly adsorbed water states. A structural model for the H₂O precursors on Fe(100) was first proposed by Anderson⁶ in a theoretical study based on an atom superposition and electron delocalization (ASED) method within a Fe₅ cluster representation. In this model, the water molecule is adsorbed on the bridge site in an upright configuration with the oxygen atom down [see Fig. 1(b)]. An activation barrier of ~0.4 eV was predicted for the dissociation of the adsorbed H₂O state into H and OH species but the stability of the precursor state with respect to its translational and rotational degrees of freedom was not examined in the study of Anderson.⁶ In later density-

functional theory (DFT) calculations, Eder *et al.*⁷ demonstrated that the upright molecular configuration adsorbed on the bridge site is the lowest-energy state of all molecular configurations they examined, but is unstable with respect to an intramolecular relaxation into dissociation, leading to a conclusion that, at low coverages, water molecules dissociate spontaneously into H and OH species. This barrierless dissociation picture is contrary not only to the prediction for a finite dissociation barrier in the ASED study⁶ but also to the EELS evidence of stable molecular species on Fe(100) at 100 K.⁵ In addition, the proposed upright H₂O configuration on the bridge site of Fe(100) is not in line with the adsorption picture that water molecule prefers a flat-lying configuration on the top site of metal surfaces [see Fig. 1(c)], established by recent theoretical studies on Ru, Rh, Pd, Pt, Al, Cu, Ag, and Au surfaces.⁸⁻¹¹ Such a flat-lying H₂O configuration on Fe(100) was not considered in the previous theoretical studies,^{6,7} which calls for more extensive theoretical studies for a proper understanding of the initial stages of water adsorption on the Fe(100) surface.

In this paper, we investigate the possibility of stable molecular states and their dissociation processes for the adsorption of a single H₂O molecule on Fe(100) by using DFT calculations. We find that there exists one locally stable molecular state on Fe(100) with an adsorption energy of 0.39

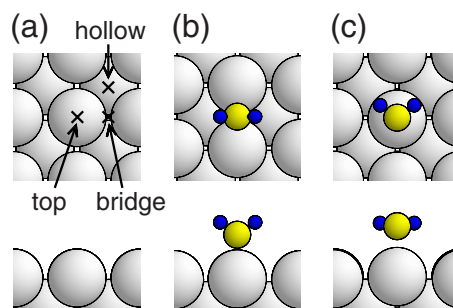


FIG. 1. (Color online) Schematic of water molecular structures on Fe(100): (a) the clean Fe(100), (b) the bridge-site upright configuration, and (c) the top-site flat-lying configuration. Balls represent Fe, O, and H atoms with decreasing size.

eV, where the H_2O molecule adsorbs on top of a surface Fe atom in a flat-lying molecular configuration. This molecular state is a precursor to more stable dissociation states, which are driven by a dissociation of H_2O into $\text{H}+\text{OH}$ with an activation barrier of 0.35 eV and a dissociation of OH into $\text{H}+\text{O}$ with a barrier of 0.79 eV. The present theory explains well the adsorption picture suggested by the previous EELS study but differs from the previous DFT study predicting a barrierless $\text{H}+\text{OH}$ dissociation of water molecule. The origin of the difference between the present and previous DFT studies will be discussed based on our test calculations.

II. METHOD

We perform DFT calculations using the Vienna *ab initio* simulation package.¹² Exchange and correlation is treated by the generalized gradient approximation allowing spin polarization,¹³ and electron-ion interaction is described by the projector augmented wave method.^{14,15} We expand the electronic wave functions in a plane-wave basis set of 29.4 Ry. The Fe(100) surface is simulated by a periodic slab geometry where each slab consists of five atomic layers and the vacuum spacing is ~ 13 Å. We employ a (3×3) surface unit cell to represent an isolated molecule, which gives a large enough intermolecular distance of ~ 8.5 Å. A single water molecule is adsorbed on the top of the slab and the contact potential difference arising from the use of an asymmetric slab is corrected by using the correction scheme of Neugebauer and Scheffler.¹⁶ Brillouin-zone integrations are done with a $4 \times 4 \times 1$ k -point mesh. All atoms but the bottom two Fe layers held at bulk positions are relaxed until the residual force components are within 0.05 eV/Å. The calculated lattice constant 2.83 Å, bulk modulus 1.77 Mbar, cohesive energy 5.17 eV, and magnetic moment $2.21\mu_B$ for bulk Fe are in good agreement with the experimental values 2.87 Å, 1.68 Mbar, 4.28 eV, and $2.22\mu_B$, respectively.¹⁷ The molecular adsorption energies calculated with the used slab thickness, k mesh, and plane-wave energy were found to converge within 0.02 eV. We determine the energy barriers for the water dissociation processes by using the climbing image nudged elastic band (CI-NEB) method,¹⁸ which is an improved version of the NEB method¹⁹ for finding minimum energy reaction paths. By construction, the CI-NEB method is designed to make one of the intermediate states near the transition point climb up along the reaction path to reach the highest saddle point, and thus results in a more accurate es-

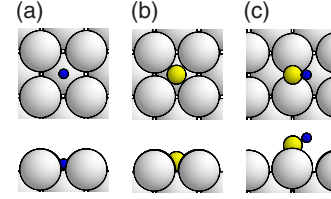


FIG. 2. (Color online) Equilibrium geometries of water dissociation products on Fe(100): (a) H, (b) O, and (c) OH species.

timization of the activation energy than the regular NEB method does, as was well demonstrated in the study of the CH_4 dissociation on Ir(111).¹⁸

III. RESULTS

We begin with the adsorption properties of the dissociated H, O, and OH species, which will serve as a basis for studying the water dissociation process. Figure 1(a) shows the top, bridge, and hollow sites of the Fe(100) surface, which compete for the adsorption of H, O, and OH. The energy minimum adsorption configurations and their structural details are summarized in Fig. 2 and Table I, respectively. For the H species, the hollow site is the most stable, the bridge site is slightly less stable by 0.03 eV than the hollow site, and the top site is locally unstable. This result is in agreement with previous DFT results that the hollow site is the most stable or almost equally stable as the bridge site^{7,20,21} and also with an EELS prediction for the hollow site.²² The H species adsorbed on the hollow site has a surface height of 0.38 Å, an adsorption energy of 0.42 eV, and a diffusion barrier of 0.11 eV. Next, for the O species, only the hollow site is locally stable, and the bridge and top sites are locally unstable. Previous DFT studies also reported that the hollow site is the most energetically stable^{7,23} and an EELS experiment suggested that oxygen atoms occupy the hollow site.²⁴ The O species adsorbed on the hollow site has a surface height of 0.61 Å, a large adsorption energy of 3.47 eV, and a high diffusion barrier of 0.66 eV. Finally, for the OH species, we find that the bridge site is the most stable, the hollow site is less stable by 0.10 eV than the bridge site, and the top site is locally unstable. The preference for the bridge site is in accordance with the DFT study of Eder *et al.*⁷ The OH species adsorbed on the bridge site has an oxygen-down configuration in which the O height is 1.59 Å, the O-H bond length is 0.98 Å, almost identical to 0.99 Å of free OH molecule, and

TABLE I. Structural parameters, adsorption energy, and diffusion barrier for water dissociation products on Fe(100). z (Å) represents the vertical height of the given atoms from the first Fe layer, the height of which is averaged over all atoms in the layer. Δx (Å) represents the lateral displacement of the given atoms from the adsorption site. $d_{\text{O-H}}$ (Å) represents the bond length between the O and H atoms. ϕ_{OH} (degree) represents the angle between the O-H bond and the surface normal. E_a (eV) represents the adsorption energy, given as the energy gain per H, O, and OH species relative to free H_2 , O_2 , and OH molecule, respectively. E_d (eV) represents the surface diffusion barrier.

Species	Adsorption site	z_{H}	Δx_{H}	z_{O}	Δx_{O}	$d_{\text{O-H}}$	ϕ_{OH}	E_a	E_d
H	Hollow	0.38	0					0.42	0.11
O	Hollow			0.61	0			3.47	0.66
OH	Bridge			1.59	0.04	0.98	60.6	3.95	0.15

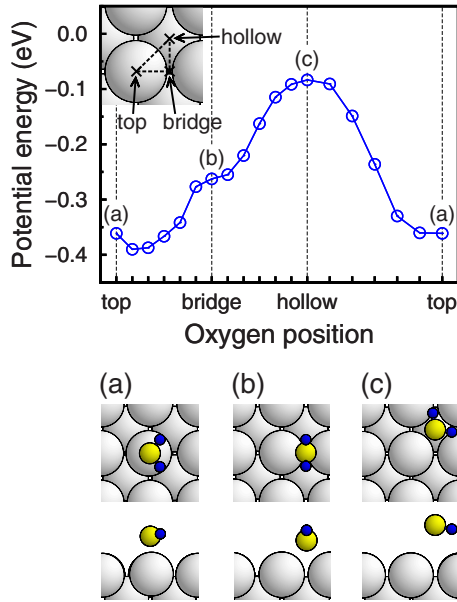


FIG. 3. (Color online) Energy diagram for the molecular adsorption of water on Fe(100). The energies are given as a function of the position of oxygen atom as indicated by dashed lines in the inset. Atomic geometries at three high-symmetry sites are displayed: (a) top, (b) bridge, and (c) hollow.

the O-H bond is tilted by 60.6° from the surface normal. The inclination of the O-H bond leads to a slight lateral displacement of the O atom, 0.04 \AA , toward the hollow site below the H atom. The adsorption energy is 3.95 eV and the diffusion barrier is 0.15 eV .

We next consider the adsorption of a H_2O molecule on the Fe(100) surface. Our first concern is to identify locally stable molecular states, which requires more careful energetics examinations for adsorption sites and molecular configurations because the H_2O molecule is expected to rather weakly interact with the surface and has more structural degrees of freedom as a triatomic molecule, compared to the dissociation species, H, O, and OH. We extend the site search into the positions on the lines connecting the high-symmetric top, bridge, and hollow sites (see the inset of Fig. 3) and, at each adsorption site, determine the lowest-energy configuration among the equilibrium structures derived from four different initial H_2O configurations: the flat-lying, the upright, and

their variants azimuthally rotated about the normal axis penetrating the O atom. Figure 3 shows the resulting energy diagram, displaying only one locally stable molecular structure. This molecular state forms a flat-lying configuration and is basically on the top site, but a little shifted toward the bridge site, reflecting the asymmetry of the molecular configuration [see the equilibrium geometry of Fig. 6(a)]. The structural and energetical details of the molecular state are summarized in Table II. The lateral displacement and surface height of the O atom are 0.35 \AA and 2.29 \AA , respectively, and the angle between the molecular plane and the surface is 10.5° . The O-H bond length 0.98 \AA and the H-O-H bond angle 105.1° are almost identical to 0.97 \AA and 104.7° of free H_2O molecule. The adsorption energy 0.39 eV indicates a weak molecule-surface interaction, and the molecular state may diffuse easily with a low barrier of 0.13 eV , passing through the bridge sites as a transition state.

Let us examine vibrational properties of the molecular adsorption structure and compare them with the water-induced EELS peaks reported by Hung *et al.*⁵ We calculated the vibration frequencies within the harmonic approximation using a displacement of $\pm 0.02 \text{ \AA}$ for the H and O atoms and the Fe atom bonded to the O atom (see Table III). In our test calculations for free H_2O molecule, the frequencies for the scissoring, O-H symmetric stretching, and O-H asymmetric stretching modes compare well with experimental data.²⁵ For the adsorbed H_2O molecule on Fe(100), we focus on the vibrational modes in the ranges of $200\text{--}4000 \text{ cm}^{-1}$ in order to compare with the EELS features at 420 cm^{-1} , 1600 cm^{-1} , and 3590 cm^{-1} , which were assigned as the Fe-O stretching, scissoring, and O-H stretching modes, respectively, of the adsorbed H_2O molecules.⁵ Our calculations support the EELS assignments of the peaks at 1600 cm^{-1} and 3590 cm^{-1} to the scissoring and O-H stretching modes, respectively. The EELS peak at 420 cm^{-1} was previously assigned to the Fe-O stretching mode, but, in our calculations, it is better assigned to the wagging modes (430 and 438 cm^{-1}). Our calculations predict the Fe-O stretching mode to appear at a much lower frequency of 217 cm^{-1} : it is likely that this low-frequency mode was buried in the strong elastic peak in the EELS spectrum (see Fig. 3 of Ref. 5). Thus, in our vibrational analysis, the EELS peaks observed at low temperatures and their vibrational modes are successfully described by the determined H_2O molecular state on Fe(100).

TABLE II. Structural parameters, adsorption energy, and diffusion barrier for a water molecule on Fe(100). $\phi_{\text{H}_2\text{O}}$ and $\phi_{\text{H-O-H}}$ (degree) represent the angle between the H_2O molecular plane and the surface and the H-O-H bond angle, respectively. The adsorption energy is given relative to free H_2O molecule. The bridge-site structure is not locally stable but is included for comparison with previous DFT and ASED calculations.

Methods	Adsorption site	z_{O}	Δx_{O}	$d_{\text{O-H}}$	$\phi_{\text{H}_2\text{O}}$	$\phi_{\text{H-O-H}}$	E_a	E_d
Present DFT	Top	2.29	0.35	0.98	10.5	105.1	0.39	0.13
	Bridge	2.01	0	0.98	90	108.5	0.26	
Previous DFT ^a	Bridge	1.87	0	1.01	90	111	0.35	
Previous ASED ^b	Bridge	1.1	0		90		2.10	

^aReference 7.

^bReference 6.

TABLE III. Calculated vibrational properties of H₂O. The frequencies are given in cm⁻¹. The experiment (Ref. 5) was performed at the temperature of 100 K and the water exposure of 0.05 L.

Systems	Methods	Stretching (Fe-OH ₂)	Wagging (H-O-H)			Stretching (O-H)	
			Symm	Asymm	Scissoring(H-O-H)	Symm	Asymm
Free H ₂ O	Present theory				1577	3718	3833
	Experiment ^a				1595	3657	3756
H ₂ O/Fe(100)	Present theory	217	430	438	1547	3550	3655
	Experiment ^b		420	420	1600	3590	3590

^aReference 25.

^bReference 5.

Figure 4 shows the projected density of states (PDOS) of the molecular adsorption structure in comparison with those of free H₂O molecule and the clean Fe(100) surface. The molecular orbitals, denoted as $1b_1$, $3a_1$, and $1b_2$, are known to have an oxygen lone-pair character perpendicular to the molecular plane, a mixture of partial lone-pair character parallel to the molecular plane and partial O-H bonding character, and an O-H bonding character, respectively.²⁶ Upon adsorption on Fe(100), the molecular orbitals undergo noticeable changes in binding energy: the $1b_1$ and $3a_1$ orbitals shift to lower energies by 0.78 (0.61) eV and 0.45 (0.33) eV, respectively, for majority- (minority-) spin part, and the $1b_2$ orbital shifts to a higher energy by 0.10 (0.13) eV. The

largest energy gain for $1b_1$ indicates that the H₂O/Fe(100) surface is stabilized by the interaction of the oxygen lone-pair electrons with the surface, as clearly seen in the charge character of a representative $1b_1$ state [see Fig. 4(b)]. This is consistent with the result of previous DFT studies on the H₂O/Pt(111) (Ref. 8) and H₂O/Cu(100) (Ref. 10) surfaces that water molecules interact with the surface through its $1b_1$ orbital. The water adsorption little affects the Fe-derived PDOS peaks but introducing weak features overlapping with the $1b_1$ and $3a_1$ levels, the character of which is found to be Fe d states. Thus, the H₂O molecular adsorption on Fe(100) is naturally understood as a weak interaction between the oxygen lone pair and the Fe d electrons.

While it is in accordance with the H₂O configurations predicted for a variety of metal surfaces (Ru, Rh, Pd, Pt, Al, Cu, Ag, and Au),⁸⁻¹¹ the present flat-lying H₂O configuration on the top site of Fe(100) differs from the bridge-site upright configuration proposed by the previous ASED (Ref. 6) and DFT (Ref. 7) studies. In the present calculations, the bridge-site upright structure was shown to be locally unstable with respect to a relaxation toward the top site: it is just a saddle-point configuration [see Fig. 3(b)]. Nonetheless, we include its adsorption properties in Table II for comparison with the previous theoretical results. The present results somewhat differ from those of the similar DFT calculations by Eder *et al.*,⁷ especially for the height of the O atom: our value 2.01 Å is much higher than their 1.87 Å. A part of this height difference is attributed to the use of different unit cells. A smaller (2×2) unit cell was used in Ref. 7. We found that our calculation using the (2×2) unit cell results in a height of 1.95 Å, much reduced from 2.01 Å in the (3×3) unit cell. The earlier ASED study of Anderson⁶ reported too low an O height of 1.1 Å and too large an adsorption energy of 2.10 eV, possibly indicating that the molecule-surface interaction was overestimated by simulating the Fe(100) surface with the use of too reactive Fe₅ cluster.

Let us consider the dissociation of the H₂O molecular state into H and OH species. Many different dissociation pathways are possible depending on final dissociation configurations. Based on our search for the energetically favored H+OH configurations, we examined four probable dissociation pathways shown in Fig. 5. In our CI-NEB calculations for the potential-energy surfaces, we found that the path shown in Fig. 5(d) has a noticeably low dissociation barrier of 0.35 eV while the paths shown in Figs. 5(a)–5(c) have as

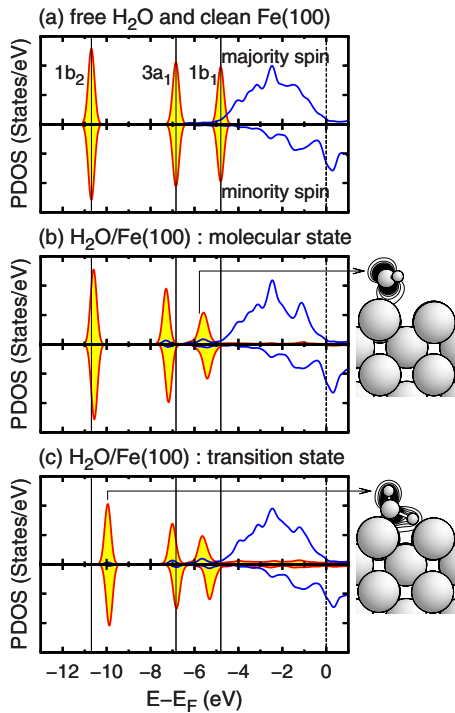


FIG. 4. (Color online) PDOS for the H₂O molecule and the top-layer Fe atom bonded to H₂O in different environments: (a) free H₂O and the clean Fe(100) surface, (b) the H₂O/Fe(100) surface (the molecular state), and (c) the H₂O/Fe(100) surface (the transition state). Shaded (solid) lines represent the PDOS for water (Fe) orbitals. Vertical solid lines represent the peak positions of the free H₂O molecule. In (b) and (c), the charge characters of representative $1b_1$ and $1b_2$ orbitals are displayed, respectively.

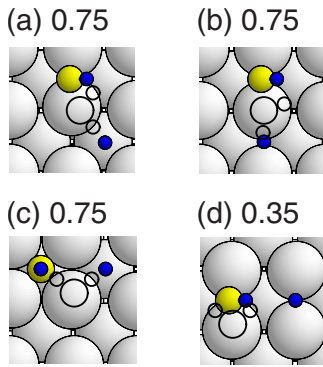


FIG. 5. (Color online) Four water dissociation paths considered in this study. Open circles represent initial molecular configurations and balls represent their final configurations. The numbers represent the dissociation barriers given in electron volt.

high a barrier as 0.75 eV via a common transition state. Figure 6 shows the detailed potential-energy curve along the lowest-barrier dissociation path shown in Fig. 5(d). The H_2O molecule that was initially on the top site migrates to an adjacent bridge site where its H atoms can closely interact with nearby Fe atoms. At the transition state found in between the bridge and hollow sites, the O-H bond breaking occurs with an energy barrier of 0.35 eV, leading to the final dissociation state in which the H and OH species occupy two neighboring bridge sites as shown in Fig. 6(c). This final state was found to be the most energetically stable in all H + OH configurations we tried by several combinations of nearby hollow- and bridge-site occupations by H and OH: its adsorption energy of 1.21 eV is larger than the values 0.99–1.18 eV for the other configurations.

It is interesting to see the electronic structure of the H_2O molecule upon dissociation. Figure 4(c) shows the PDOS of the transition state for the dissociation process. Here, the $1b_2$ orbital undergoes a noticeable change in peak position with respect to the equilibrium molecular state: a high-energy shift of 0.65 (0.69) eV for majority (minority) spin. Since the $1b_2$ level corresponds to the O-H bonding orbital, its destabilization indicates a weakening of the O-H bond during the dissociation process, as well displayed in the charge character of a representative $1b_2$ state in Fig. 4(c). Only a small change in the $1b_1$ level implies that the oxygen lone-pair-mediated molecular bonding is preserved until the O-H bond breaking.

The energy barrier 0.35 eV corresponds to dissociation temperatures of 118–136 K, when estimating by assuming an Arrhenius-type activation process with use of the attempt frequency ranging from 10^{13} to 10^{15} Hz. This estimation agrees qualitatively with the EELS report for a low exposure (0.1 L) that the characteristic spectra indicating the hydroxyl

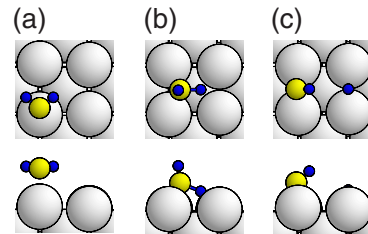
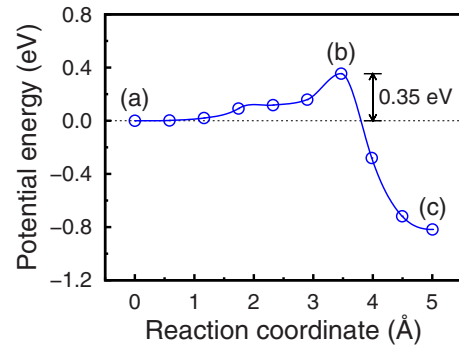


FIG. 6. (Color online) Energy diagram for the lowest-barrier dissociation of water molecule on Fe(100). Three representative configurations marked in the diagram are displayed: (a) initial H_2O precursor state, (b) transition state, and (c) final H + OH dissociated state.

species appear when heating to 178 K.⁵ On the other hand, the present finite-barrier dissociation picture is contrary to the DFT result of Eder *et al.*⁷ that predicted a barrierless dissociation. This difference is somewhat interesting because the reaction paths examined in both DFT studies are almost the same: they examined a dissociation path from the initial structure of Fig. 1(b) to the final structure of Fig. 6(c). Our independent calculations imply that the result of a barrierless dissociation by Eder *et al.* was possibly due to an underestimation of the barrier in their NEB calculations. We tried the path examined by Eder *et al.* using the reduced (2×2) unit cell and found that, while the CI-NEB method gives a barrier of 0.25 eV, the NEB method results in a barrier as low as 0.05 eV. This result stresses that an accurate determination of energy barrier requires more rigorous transition-state searching schemes going beyond the usual NEB method, as was demonstrated before in the study of the $\text{CH}_4/\text{Ir}(111)$ surface.¹⁸

The adsorption properties of the H + OH state shown in Fig. 6(c) are summarized in Table IV. Our calculations appear to be somewhat different from the DFT results of Eder *et al.*, especially for the heights of O and H but it was also confirmed in our calculations that the use of different unit cells is the origin of such differences. It is noticeable in the calculated energetics for the H + OH configurations that the OH species always favor the bridge site over the hollow site

TABLE IV. Structural parameters and adsorption energy for the H + OH state shown in Fig. 6(c).

Methods	z_{O}	Δx_{O}	$d_{\text{O-H}}$	ϕ_{OH}	z_{H}	Δx_{H}	E_{a}
Present DFT	1.56	0.17	0.98	51.0	1.09	0.01	1.21
Previous DFT ^a	1.47		1.01	64	0.99		1.13

^aReference 7.

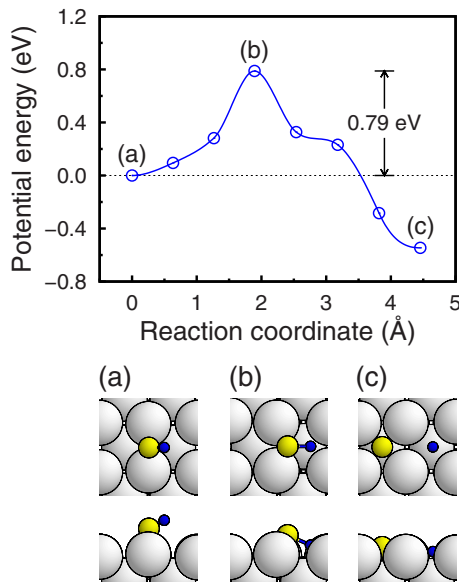


FIG. 7. (Color online) Energy diagram for the dissociation of OH on Fe(100). Three representative configurations marked in the diagram are displayed: (a) initial OH state, (b) transition state, and (c) final H+O dissociated state.

regardless of which site is occupied by the H species. This result confirms the EELS report that the dissociated OH species occupy the bridge site.⁵ It was also suggested, based on the EELS spectra measured at an off-specular angle, that the OH species is tilted from the surface normal. In our calculations, the OH species adsorbed on the bridge sites are tilted by 37° – 51° from the surface normal.

The adsorbed OH species is also subject to a further dissociation. Here, for simplicity, we only consider the dissociation of an isolated OH group: we neglect the influence of the H species, the other dissociation product of water molecule. Such a nearby H species is not likely because the H and OH species are expected to readily diffuse with increasing temperature due to their low diffusion barriers of 0.11–0.15 eV (see Table I). The dissociation path we considered is shown in Fig. 7. The OH group that was initially adsorbed on a bridge site dissociates into H+O species, occupying the nearby hollow sites which were verified before to be the most stable for both H and O species. The CI-NEB calculations result in an energy barrier of 0.79 eV. This barrier height corresponds to temperatures of 265–306 K in our Arrhenius-type analysis, which compares well with ~ 310 K reported for the OH dissociation by the TPD experiment.⁵ After the full decomposition, the H and O atoms are expected to occupy the hollow sites, which are known as the most stable for individual H and O species. It was found that the interaction between the adsorbed H and O species are

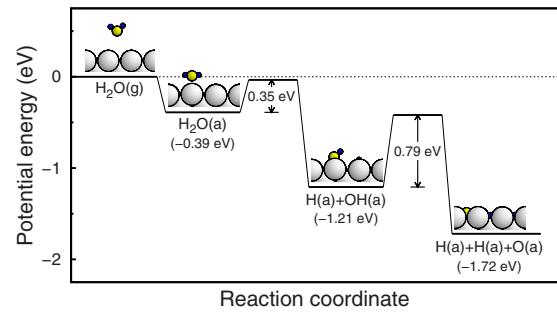


FIG. 8. (Color online) Reaction energy diagram for a single H_2O molecule on Fe(100).

negligible, i.e., the adsorption energy appears insensitive to the distribution of individual H and O atoms: in our (3×3) unit-cell calculations, a dense configuration of the H and O atoms appears to be equally stable as a sparse configuration with an energy difference less than 0.01 eV. For the atomic diffusions, the H species with a lower diffusion barrier (0.11 eV) will diffuse more readily than the O species (0.66 eV).

Figure 8 illustrates the whole dissociation process of a single H_2O molecule on the Fe(100) surface. The incoming H_2O molecule prefers to adsorb with no barrier on top of a surface Fe atom with an energy gain of 0.39 eV. The adsorbed H_2O can easily dissociate into H+OH by overcoming a low-energy barrier of 0.35 eV. The dissociated H and OH species energetically favor the adsorption on a pair of adjacent bridge sites with an adsorption energy of 1.21 eV but easy diffusions are likely to drive them apart from each other. The OH species dissociates further into H+O by overcoming an energy barrier of 0.79 eV. After a full dissociation, the individual H and O species prefer to adsorb individually on the hollow sites, and the total-energy gain by dissociation is about 1.72 eV relative to free H_2O molecule.

IV. SUMMARY

The present DFT calculations for a single H_2O molecule on the Fe(100) surface have identified a molecular precursor state, which is in a flat-lying molecular configuration on the top site and is subject to a low-barrier dissociation into H+OH. This precursor-mediated dissociation channel, which was overlooked in earlier theoretical studies, and the resulting energy diagram for the $\text{H}_2\text{O}/\text{Fe}(100)$ surface offers a unified theoretical picture well explaining the EELS and TPD measurements at low water exposures.

ACKNOWLEDGMENTS

This work was supported by the POSTECH Steel Science Research Program funded by POSCO (Grant No. 2008Y239).

- ¹J. M. Heras and L. Viscido, *Catal. Rev. - Sci. Eng.* **30**, 281 (1988).
- ²V. E. Henrich and P. A. Cox, *Appl. Surf. Sci.* **72**, 277 (1993).
- ³G. E. Brown, Jr., V. E. Henrich, W. H. Casey, D. L. Clark, C. Eggleston, A. Felmy, D. W. Goodman, M. Grätzel, G. Maciel, M. I. McCarthy, K. H. Nealson, D. A. Sverjensky, M. F. Toney, and J. M. Zachara, *Chem. Rev.* **99**, 77 (1999).
- ⁴D. J. Dwyer, G. W. Simmons, and R. P. Wei, *Surf. Sci.* **64**, 617 (1977).
- ⁵W.-H. Hung, J. Schwartz, and S. L. Bernasek, *Surf. Sci.* **248**, 332 (1991).
- ⁶A. B. Anderson, *Surf. Sci.* **105**, 159 (1981).
- ⁷M. Eder, K. Terakura, and J. Hafner, *Phys. Rev. B* **64**, 115426 (2001).
- ⁸A. Michaelides, V. A. Ranea, P. L. de Andres, and D. A. King, *Phys. Rev. Lett.* **90**, 216102 (2003).
- ⁹A. Michaelides, V. A. Ranea, P. L. de Andres, and D. A. King, *Phys. Rev. B* **69**, 075409 (2004).
- ¹⁰S. Wang, Y. Cao, and P. A. Rikvold, *Phys. Rev. B* **70**, 205410 (2004).
- ¹¹J. Li, S. Zhu, Y. Li, and F. Wang, *Phys. Rev. B* **76**, 235433 (2007).
- ¹²G. Kresse and J. Furthmüller, *Phys. Rev. B* **54**, 11169 (1996).
- ¹³J. P. Perdew, in *Electronic Structure of Solids '91*, edited by P. Ziesche and H. Eschrig (Akademie Verlag, Berlin, 1991).
- ¹⁴P. E. Blöchl, *Phys. Rev. B* **50**, 17953 (1994).
- ¹⁵G. Kresse and D. Joubert, *Phys. Rev. B* **59**, 1758 (1999).
- ¹⁶J. Neugebauer and M. Scheffler, *Phys. Rev. B* **46**, 16067 (1992).
- ¹⁷C. Kittel, *Introduction to Solid State Physics*, 8th ed. (Wiley, New York, 2005).
- ¹⁸G. Henkelman, B. P. Uberuaga, and H. Jónsson, *J. Chem. Phys.* **113**, 9901 (2000).
- ¹⁹H. Jónsson, G. Mills, and K. W. Jacobsen, in *Classical and Quantum Dynamics in Condensed Phase Simulations*, edited by B. J. Berne, G. Ciccotti, and D. F. Coker (World Scientific, Singapore, 1998).
- ²⁰D. E. Jiang and E. A. Carter, *Phys. Rev. B* **70**, 064102 (2004).
- ²¹D. C. Sorescu, *Catal. Today* **105**, 44 (2005).
- ²²P. B. Merrill and R. J. Madix, *Surf. Sci.* **347**, 249 (1996).
- ²³P. Błoński, A. Kiejna, and J. Hafner, *Surf. Sci.* **590**, 88 (2005).
- ²⁴J.-P. Lu, M. R. Albert, S. L. Bernasek, and D. J. Dwyer, *Surf. Sci.* **215**, 348 (1989).
- ²⁵D. Elsenberg and W. Kauzmann, *The Structure and Properties of Water* (Oxford University Press, New York, 1969).
- ²⁶P. A. Thiel and T. E. Madey, *Surf. Sci. Rep.* **7**, 211 (1987).